Self-Assembly of Charge Stabilized Colloidal Nanoparticles

Eric M. Janke[1], Trung Nguyen[2], Monica Olvera de la Cruz[2], Dmitri V. Talapin[1]

[1]Department of Chemistry and James Franck Institute, University of Chicago, Chicago, IL 60637

[2]Department of Chemistry, Northwestern University, Evanston, IL 60208

Introduction

We report an investigation of force fields around electrostatically stabilized colloidal nanoparticles elucidating the relationship between dielectric properties of the nanoparticle material and their flocculation and assembly behavior. Dielectric polarization effects have been predicted to have a strong effect[1] on double electric layers that form around colloidal nanoparticles in charge-asymmetric electrolyte solutions. We focus on colloidal nanoparticles that are stabilized by compact chalcogenidometallate (ChM) anions. Flocculation of such colloids by controlled addition of excess ChM salts results in loss of colloidal stability. For dielectric particles, the resulting aggregates are loose and open while for colloidal metal particles, we observe growth of self-assembled superlattices. Structural characterization of the resulting supercrystalline material reveals cleanly faceted structures with micron scale edge lengths and a high degree of internal order. The ChM ligands are found to decompose and cross-link, forming an amorphous glassy metal chalcogenide matrix that fills the interstices of the ordered nanocrystal array. We further study the mechanism of the crystallization process that leads to formation of our supercrystals and find that the ordered phase appears by particles first agglomerating into a dense amorphous phase, and then subsequently rearranging into an ordered lattice. These results validate course-grained models which predict that induced surface charges affect the short-range forces between particles differently for metallic and dielectric particles. The unique propensity for metallic nanoparticles to assemble is due to polarization effects whereby attractive image charges allow for a denser cloud of associated ChM anions to form around them. This effect in turn provides strong short-range repulsive forces that prevent jamming during the early stages of the assembly process.

Ligand Exchange and Assembly

Au nanoparticles with diameters around 5 nm were synthesized with native 1-dodecanethiol (DDT) ligands providing colloidal stability in non-polar solvents. The Au particles were then re-functionalized by a two-phase ligand exchange process. DDT capped Au particles were dispersed in toluene and phase transferred by stirring into an immiscible hydrazine solution of the salt $(N_2H_5)_4Sn_2S_6$ (Fig 1a). During the phase transfer process, surface bound anionic dodecanethiolate ligands are displaced by thiostannate in the following reaction: $4DDT_{Au} + (N_2H_5)_4Sn_2S_{6\ solution} \rightarrow Sn_2S_6^{4-}{}_{Au} + 4(N_2H_5)DDT_{solution}$ After washing steps to remove (N_2H_5)DDT, the resulting Au particles are electrostatically stabilized and net negatively charged by their capping layer of $Sn_2S_6^{4-}$ anions. Charge is balanced by free solvated protons in the form of $N_2H_5^+$. Slow addition of excess $(N_2H_5)_4Sn_2S_6$ solution to incrementally increase the concentration of unbound ligand results in flocculation of the colloidal Au. This is expected given that $(N_2H_5)_4Sn_2S_6$ is an electrolyte which dissociates into free ions in hydrazine and its addition should destabilize the colloid due to its effect on the ionic strength of the solution. Surprisingly, Au particles flocculated from hydrazine by this method assemble into ordered supercrystalline arrays (Fig 1a). Imaging of the ordered aggregates (Fig 1c,d) by TEM and SEM reveals a high degree of internal order with nanocrystal units packed into dense periodic arrays to form supercrystals with micron scale dimensions. Comparison of this material to self-assembled structures grown from DDT capped Au reveals a marked contraction (Fig 1c) in the equilibrium spacing between particles due to the compact size of the $Sn_2S_6^{4-}$ anion relative to DDT. Small-angle x-ray scattering (SAXS) measurements (Fig 1e) confirm that fcc supercrystals grown from 5 nm Au have a nearest neighbor center to center spacing shrinking from 7.5 nm for DDT capped Au down to 5.6 nm for the ligand exchanged Au assembled by flocculation from hydrazine.

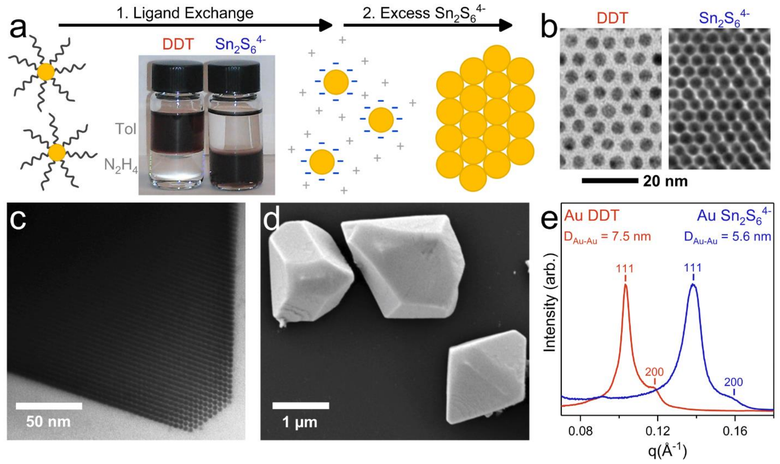

Figure 1: Ligand exchange of Au nanocrystals from native organic ligands to compact inorganic anions and subsequent self-assembly. a, A schematic depicting the ligand exchange and self-assembly processes. b, Zoomed in TEM image comparing spacing for self-assembled Au capped with DDT and $Sn_2S_6^{4-}$. c, TEM of an octahedral SC grown from $Sn_2S_6^{4-}$ capped Au. d, SEM image showing three large supercrystals of the same type in (c). e, SAXS data on a linear scale comparing the lattice spacing of assembled Au using long organic ligands and short $Sn_2S_6^{4-}$ ligands.

Polarization Effects

Image charges due to dielectric mismatch impact the distribution of ions around charge stabilized particles in polar media. In asymmetric electrolyte solutions, the dense layer of anions associated with the surface of metal particles produces short range repulsive forces that prevent jamming and allow assembly. Dielectric particles develop net-attractive pair potentials when flocculated by ChM salts and undergo the same "sticky aggregation" process as metal particles treated with 1:1 electrolytes.

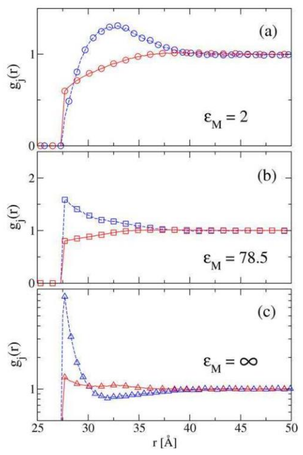

Figure 2[1]: Simulated radial distribution functions $g_j(r)$ as a function of distance, r[Å], to the center of a spherical nanoparticle. Particles are considered to be negatively charged and immersed in an aqueous 3:1 electrolyte at 0.233 M. Panels a, b, and c are computed for nanoparticles with dielectric constants of 2, 78.5 (solvent matched), and infinity. Red traces show the distribution profile of monovalent co-ions (negative) while blue traces correspond to the trivalent counterions.

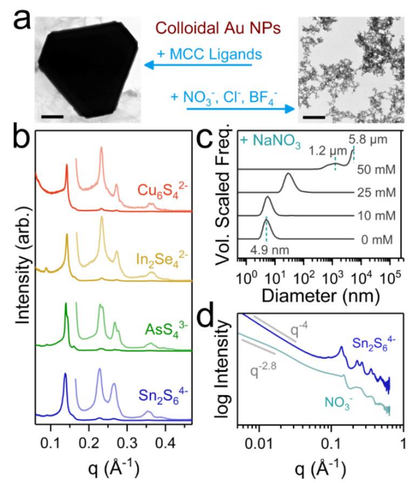

Figure 3: Generality of chalcogenidometallate based assembly of Au. a, TEM images summarizing the result of aggregating colloidal Au with MCC ligands (left) and non-binding 1:1 electrolytes (right). Scale bars are 500 nm. b, Linear scale SAXS data showing the result of assembling colloidal Au by adding different hydrazinium chalcogenidometallate salts. Light traces correspond to dark traces x20 for visibility. c, DLS data showing the uncontrolled fractal aggregation that results from addition of $NaNO_3$ to colloidal Au in N_2H_4. d, Log-log scale SAXS comparing the Porod's Law scaling at low q for Au aggregated with $NaNO_3$ and with $(N_2H_5)_4Sn_2S_6$.

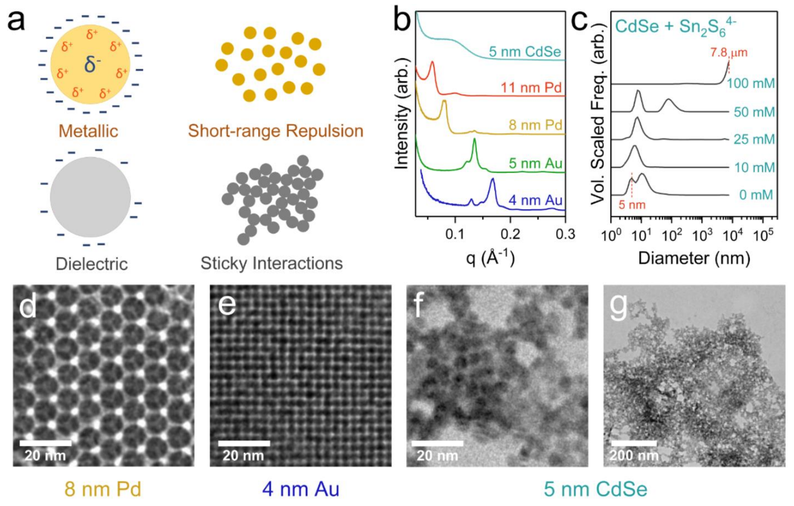

Figure 4: Role of NC core material in assembly. a, Schematic depicting the effect of dielectric polarizability of the NC core on density of associated anions and the resulting pair potentials. b, Linear scale SAXS data of particles of different sizes and core materials aggregated from N_2H_4 with $(N_2H_5)_4Sn_2S_6$. c, DLS data showing the uncontrolled fractal aggregation that results from adding $(N_2H_5)_4Sn_2S_6$ to CdSe in N_2H_4. d, TEM of (111) face of 8 nm Pd SC. e, TEM of (100) face of 4 nm Au SC. f,g. TEM of CdSe showing aggregation due to sticky short-range interactions.

Mechanism of Ordering

Au colloids flocculated by the specific method of adding excess hydrazinium chalcogenidometallate ligands retain strongly repulsive interparticle forces at short range. With particles prevented from jamming, these loose agglomerations are able to find a global energetic minimum by ordering and densifying into supercrystals. Over the timescale of hours, these suspended agglomerations first order loosely, then densify into the final supercrystalline structure as slow decomposition of the bound ligands leaves behind amorphous SnS_2 glass in the interstices. At right, an image depicts a snapshot of a course-grained simulation of the assembly process with Au NPs in brown and ChM anions in cyan.

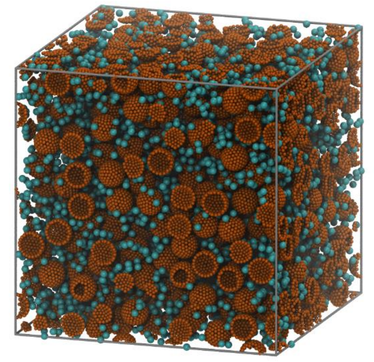

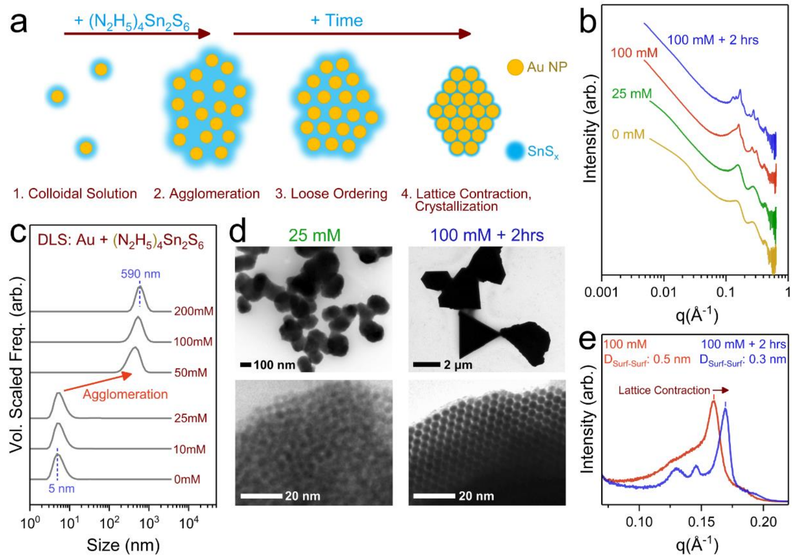

Figure 5: Mechanism of assembly of $Sn_2S_6^{4-}$ capped Au nanoparticles. a, Schematic diagram depicting the assembly process. b, SAXS data on a log-log scale showing the progression of structuring that occurs as the conc. of $(N_2H_5)_4Sn_2S_6$ is increased. c, DLS data showing the transition from the colloidal to agglomerated state that occurs between 25 and 50 mM added ligand. d, TEM images showing the material recovered from 25 and 100 mM solutions of $(N_2H_5)_4Sn_2S_6$ in hydrazine. e, Linear scale SAXS plot emphasizing the lattice contraction and ordering that occurs after the initial loose ordering stage.

References and Acknowledgements

Acknowledgement of Support:
This work was supported by MICCoM as part of the Computational Materials Sciences Program funded by the US Department of Energy (DOE), Office of Science, Basic Energy Sciences (BES), Materials Sciences and Engineering Division (5J-30161-0010A)

Reference:

1. *J. Phys. Chem. B*, **2014**, 118 (29), pp 8854–8862